1-28-2004

Comprehensive Laboratory Measurements of Biomass-Burning Emissions: 2. First Intercomparison of Open-Path FTIR, PTR-MS, and GC-MS/FID/ECD

Ted J. Christian
University of Montana - Missoula

B. Kleiss
Max Planck Institute for Chemistry

Robert J. Yokelson
University of Montana - Missoula, bob.yokelson@umontana.edu

R. Holzinger
University of California - Irvine

P. J. Crutzen
Max Planck Institute for Chemistry

Follow this and additional works at: https://scholarworks.umt.edu/chem_pubs

See next page for additional authors

Part of the Biochemistry Commons, and the Chemistry Commons

Let us know how access to this document benefits you.

Authors

Ted J. Christian, B. Kleiss, Robert J. Yokelson, R. Holzinger, P. J. Crutzen, Wein Min Hao, T. Shirai, and Donald R. Blake

Comprehensive laboratory measurements of biomass-burning emissions:
2. First intercomparison of open-path FTIR, PTR-MS, and GC-MS/FID/ECD

T. J. Christian,[1] B. Kleiss,[2] R. J. Yokelson,[1] R. Holzinger,[2,3] P. J. Crutzen,[2,4] W. M. Hao,[5] T. Shirai,[6,7] and D. R. Blake[6]

[1]   Oxygenated volatile organic compounds (OVOC) can dominate atmospheric organic chemistry, but they are difficult to measure reliably at low levels in complex mixtures. Several techniques that have been used to speciate nonmethane organic compounds (NMOC) including OVOC were codeployed/intercompared in well-mixed smoke generated by 47 fires in the U.S. Department of Agriculture Forest Service Fire Sciences Combustion Facility. The agreement between proton transfer reaction mass spectrometry (PTR-MS) and open-path Fourier transform infrared spectroscopy (OP-FTIR) was excellent for methanol (PT/FT = 1.04 ± 0.118) and good on average for phenol (0.843 ± 0.845) and acetol (~0.81). The sum of OP-FTIR mixing ratios for acetic acid and glycolaldehyde agreed (within experimental uncertainty) with the PTR-MS mixing ratios for protonated mass 61 (PT/FT = 1.17 ± 0.34), and the sum of OP-FTIR mixing ratios for furan and isoprene agreed with the PTR-MS mixing ratios for protonated mass 69 (PT/FT = 0.783 ± 0.465). The sum of OP-FTIR mixing ratios for acetone and methylvinylether accounted for most of the PTR-MS protonated mass 59 signal (PT/FT = 1.29 ± 0.81), suggesting that one of these compounds was underestimated by OP-FTIR or that it failed to detect other compounds that could contribute at mass 59. Canister grab sampling followed by gas chromatography (GC) with mass spectrometry (MS), flame ionization detection (FID), and electron capture detection (ECD) analysis by two different groups agreed well with OP-FTIR for ethylene, acetylene, and propylene. However, these propylene levels were below those observed by PTR-MS (PT/FT = 2.33 ± 0.89). Good average agreement between PTR-MS and GC was obtained for benzene and toluene. At mixing ratios above a few parts per billion the OP-FTIR had advantages for measuring sticky compounds (e.g., ammonia and formic acid) or compounds with low proton affinity (e.g., hydrogen cyanide and formaldehyde). Even at these levels, only the PTR-MS measured acetonitrile and acetaldehyde. Below a few ppbv only the PTR-MS measured a variety of OVOC, but the possibility of fragmentation, interference, and sampling losses must be considered.   *INDEX TERMS:* 0315 Atmospheric Composition and Structure: Biosphere/atmosphere interactions; 0322 Atmospheric Composition and Structure: Constituent sources and sinks; 0365 Atmospheric Composition and Structure: Troposphere—composition and chemistry; 0394 Atmospheric Composition and Structure: Instruments and techniques; *KEYWORDS:* instrument intercomparision, biomass burning, oxygenated organic compounds

[1]Department of Chemistry, University of Montana, Missoula, Montana, USA.

[2]Atmospheric Chemistry Department, Max Planck Institute for Chemistry, Mainz, Germany.

[3]Now at Department of Environmental Science, Policy and Management, University of California, Berkeley, California, USA.

[4]Also at Scripps Institution of Oceanography, University of California, San Diego, La Jolla, California, USA.

[5]Fire Sciences Laboratory, USDA Forest Service, Missoula, Montana, USA.

[6]Department of Chemistry, University of California, Irvine, California, USA.

[7]Now at Earth Observation Research Center, Japan Aerospace Exploration Agency, Tokyo, Japan.

1. Introduction

[2] It is widely accepted that detailed models are needed to quantify the complex chemistry of the atmosphere. It is also true that the output of these models is sensitive to trace gas species present at very low levels. A dramatic example of this is O^1D, a key species in atmospheric photochemical models that is present at levels so low that it may never be measured in the troposphere [*Albritton et al.*, 1990]. OH and HO_2 (collectively known as HO_x) are two other species of prime importance (largely derived from O^1D) that have been measured reliably only recently [*Mount and Williams*, 1997; *Brune et al.*, 1998].

[3] The organic chemistry of the atmosphere is of great interest for many reasons including its major influence on O_3 (and thus O^1D), HO_x, and the oxidizing efficiency (power) of the atmosphere [*Singh et al.*, 1995, 2001; *McKeen et al.*, 1997; *Mason et al.*, 2001]. Until recently, it was widely assumed that the organic chemistry of the atmosphere was well understood, mainly because hydrocarbons (which were thought to be the main organic constituents of the atmosphere) are routinely speciated at parts per billion or trillion (ppb, 10^{-9}, ppt, 10^{-12}) levels by a variety of GC-based techniques [e.g., *Blake et al.*, 1996]. The hydrocarbon/O_3 observations were reasonably consistent with atmospheric models, especially for smog chambers [*Carter et al.*, 1979] or urban airsheds [*McRae and Seinfeld*, 1983]. However, in the 1990s, it became clear that OVOC account for most of the NMOC from biomass burning [*Griffith et al.*, 1991; *Yokelson et al.*, 1996, 1997, 1999, 2003a; *Worden et al.*, 1997; *Holzinger et al.*, 1999] and a large fraction of the biogenic emissions from plants [*König et al.*, 1995; *Kirstine et al.*, 1998; *Schade and Goldstein*, 2001]. Together these sources are estimated to produce more total trace gases and more VOC than the main global trace gas source: fossil fuel burning [*Schimel et al.*, 1995; *Andreae and Merlet*, 2001; *Guenther et al.*, 1995]. In addition, the nonmethane hydrocarbons (NMHC) emitted by fossil fuel burning quickly become OVOC in the atmosphere, mainly by reaction with OH. The above observations probably help explain why recent campaigns to characterize the background troposphere found that OVOC were up to five times more abundant than NMHC [*Singh et al.*, 2001], more reactive than the NMHC [*Singh et al.*, 1995] and consequently more important. Further, current photochemical models (at various local-global scales) are unable to rationalize the simultaneous observations of PAN, acetaldehyde, etc. [*Flocke et al.*, 2002; *Chatfield et al.*, 2002; *Staudt et al.*, 2003]. This is a crucial weakness since OVOC photochemistry is a major HO_x source, especially in drier parts of the troposphere. Finally, the few initial field observations of OVOC multiphase chemistry are not explained by available chemical mechanisms [*Yokelson et al.*, 2003a]. Thus it is clear that the organic chemistry of the atmosphere is not well understood and that a great need exists for instrumentation that can reliably identify and quantify the OVOC in both field and laboratory studies. This paper describes the first informal, but rigorous, code-ployment/intercomparison of major techniques that have potential to provide broad characterization of NMOC, including OVOC. The measurements probed well-mixed smoke generated by 47 fires burned in the U.S. Department

of Agriculture (USDA) Forest Service Fire Sciences Laboratory (FSL) in Missoula, MT. Gas measurement techniques included canister sampling followed by gas chromatographic (GC) analysis (e.g., GC-mass spectrometry (MS), GC-flame ionization detection (FID), and GC-electron capture detection (ECD)) performed by two groups along with proton transfer reaction mass spectrometry (PTR-MS) and Fourier transform infrared spectrometry (FTIR). The canister techniques have been widely used for many years and provide analysis (with preconcentration) at ppt levels [*Montzka et al.*, 1993]. However, they may be subject to sampling and storage artifacts for trace gases that are unstable or sticky, which can comprise the majority of NMOC gases of interest in atmospheric chemistry studies. Open-path FTIR (OP-FTIR) is artifact-free. Since all molecules have a unique IR signature, FTIR is well suited for identification and quantification of most trace gases, but not below the ppb levels needed to probe the clean troposphere [*Goode et al.*, 1999]. PTR-MS involves no sample storage and can quantify down to tens of ppt levels virtually any volatile gas with a proton affinity (PA) moderately above that of water. However, PTR-MS provides only one signal for a mass/charge ratio that could represent several species, which makes compound identification challenging under some conditions [*Holzinger et al.*, 2000]. In summary, each technique has its strengths and weaknesses. The focus of this paper is to further quantify the capabilities of each technique by employing these methods simultaneously. A detailed discussion of the emissions from African and Indonesian fuels used in this study appears in a companion paper [*Christian et al.*, 2003].

2. Experiment
2.1. Combustion Facility

[4] The combustion facility at FSL measures 12.5 m × 12.5 m × 22 m high (Figure 1). A 1.6 m diameter exhaust stack with a 3.6 m inverted funnel opening extends from ~2 m above the floor through the ceiling. The room is pressurized with outside air that has been conditioned for temperature and humidity, and is then vented through the stack, completely entraining the emissions from fires burning beneath the funnel. The fires are burned on a continuously weighed fuel bed (80 × 210 cm). A sampling platform surrounds the stack at 17 m elevation where all the temperature, pressure, trace gas, and particle measurement equipment for this experiment was deployed except background CO_2 (LICOR 6262). A large orifice near the base of the stack promotes mixing of the emissions. Three separate tests have shown that the emissions are very well mixed in the stack at the height of the sampling platform: (1) The temperature profile across the stack at this height is "flat," even as the temperature rises and falls because of fires burning below. (2) The average mixing ratios for an optical path that spanned the stack were the same as those measured by point sampling at the stack center (for CO_2, CO, and hydrocarbons) [*Goode et al.*, 1999]. (3) The mixing ratios for reactive or sticky species were constant across the width of the stack, as determined by quickly moving the inlet for the PTR-MS to different positions within the stack (Figure 2). The fuel selection criteria for African, Indonesian, and other fuels; fuel sampling and fuel
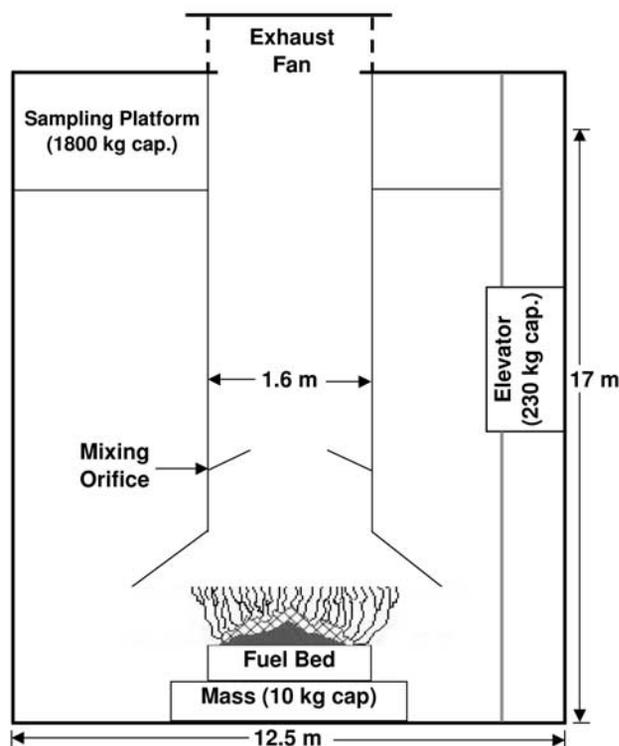
Figure 1. A schematic diagram of the USDA Forest Service Fire Sciences Laboratory combustion facility. All measurements except background CO_2 were made in well-mixed smoke from the sampling platform.

characterization methodology; and fire simulations are described in detail in the companion paper [*Christian et al.*, 2003].

2.2. Trace Gas and Particle Instrumentation

2.2.1. Open-Path FTIR

[5] The open-path Fourier transform infrared spectrometer (OP-FTIR) was positioned on the sampling platform so that the open white cell spanned the stack directly in the rising emissions stream for continuous (0.83 s resolution) scanning. The OP-FTIR system [*Yokelson et al.*, 1997] includes a MIDAC model 2500 spectrometer; a 1.6 m base path, open White cell; and an MCT (mercury-cadmium-telluride), LN_2-cooled detector. The path length was set to 57.7 m and spectral resolution was 0.5 cm^{-1}. All spectra were saved in real time on a computer synchronized with the rest of the data acquisition. Before each fire, we scanned for 2–3 min to obtain a background spectrum, and then we made absorbance spectra for each scan during the fire at 0.83 s resolution using the appropriate background spectrum. For long-duration fires (∼1–3 hours) with slowly changing temperature and emissions, we increased the signal-to-noise ratio (S/N) by averaging up to 72 absorbance spectra (∼1 min resolution). For shorter fires with larger or more rapid temperature fluctuations, averaging was limited to 7 spectra (∼6 s resolution).

[6] We used classical least squares spectral analysis [*Griffith*, 1996; *Yokelson and Bertschi*, 2002; *Yokelson et al.*, 1996] to retrieve excess mixing ratios for water (H_2O), methane (CH_4), methanol (CH_3OH), ethylene (C_2H_4), phe-

nol (C_6H_5OH), acetone ($CH_3C(O)CH_3$), acetol ($CH_2(OH)C(O)CH_3$), isoprene (C_5H_8), hydrogen cyanide (HCN), acetylene (C_2H_2), furan (C_4H_4O), nitric oxide (NO), and formaldehyde (HCHO). We used spectral subtraction [*Yokelson et al.*, 1997] to retrieve excess mixing ratios for water (H_2O), ammonia (NH_3), formic acid (HCOOH), acetic acid (CH_3COOH), glycolaldehyde ($CH_2(OH)CHO$), propylene (C_3H_6), and methylvinylether (MVE, CH_3OCHCH_2). While CO_2 and CO are accurately measured by OP-FTIR [*Goode et al.*, 1999], because of the large volume of data, we opted to use the convenient, synchronized data for these molecules from the real-time instruments (vide infra). The molecules discussed above account for all the significant, sharp (i.e., FWHM < ∼5 cm^{-1}) features observed from 600–3400 cm^{-1} in all the IR spectra. The detection limit for most gases was 5–20 ppb for a 1-min measurement time and ∼10–50 ppb at the highest time resolution used (6 s). The typical uncertainty in an FTIR mixing ratio is ±5% (1σ) because of calibration or the detection limit (2σ), whichever is greater.

[7] The advantages of OP-FTIR trace gas measurements include the following: (1) no possibility of sampling or
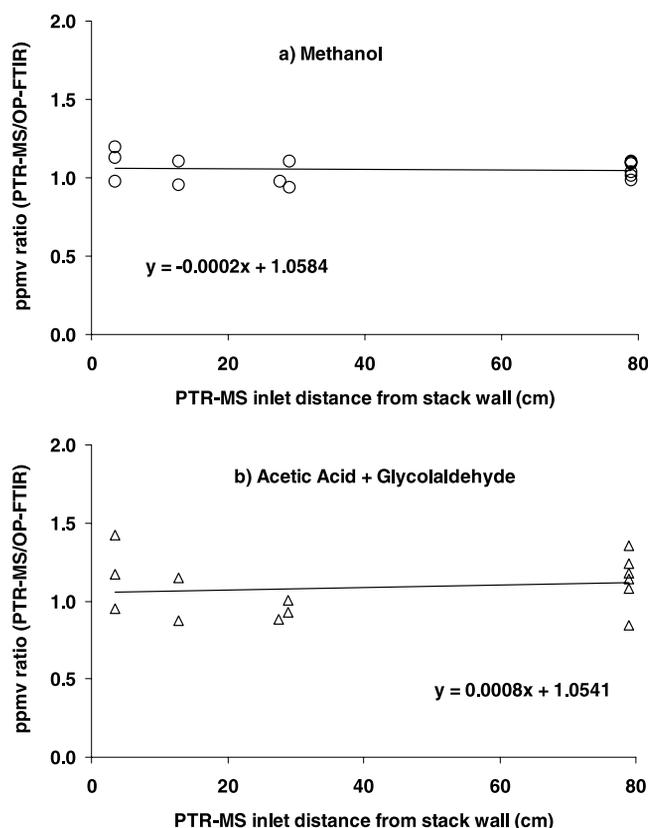
Figure 2. (a) Ratio of PTR-MS methanol (point-source) to OP-FTIR methanol (path integrated) as the PTR inlet is repeatedly moved from the center of the stack (80 cm) to within 4 cm of the stack wall. The ratio is independent of position, which indicates that the smoke is well mixed. (b) No position dependence was observed for acetic acid, which is a stickier compound. Rapid switching between two PTR-MS inlets, one of which was filtered with a Teflon filter, also had no measurable effect, indicating that particles did not interfere with the trace gas measurements.

storage artifacts since there is no sampling, (2) excellent compound identification and resistance to interference since most molecules have multiple, unique features, (3) simultaneous quantification of a large number of reactive or stable, organic or inorganic molecules at high ($\sim$1 s) temporal resolution and ppb-percent levels, (4) unanticipated compounds can be quantified, and (5) reduction of the uncertainty that can be associated with point sampling since the optical path can be adjusted to integrate over the whole phenomenon being investigated. The main disadvantages of FTIR are: (1) a nonlinear response for some species, which requires a time-consuming analysis [*Yokelson and Bertschi*, 2002], (2) weak IR features for homonuclear diatomic molecules (e.g., H_2 and N_2), some sulfur molecules (e.g., H_2S), and a few other molecules, (3) some molecules strong IR features are overlapped, under most tropospheric conditions, by much stronger water lines (e.g., CH_3Cl, glyoxal, and acetaldehyde), and (4) ppb detection limits (when preconcentration is not used), which are inadequate for most molecules in clean air (limited by IR source stability). FTIR detection limits can be in the ppt range with preconcentration [*Hanst et al.*, 1975], but then the advantages for quantifying reactive and sticky compounds may be lost.

2.2.2. PTR-MS

[8] The PTR-MS sampled continuously from the emissions stream through $\sim$2 m of 6 mm i.d. Teflon tubing that opened directly above the center of the OP-FTIR optical path. It was established at the outset that moving the inlet did not affect the results (Figure 2), nor did placement of a Teflon filter over the inlet entrance. The sample line was short to minimize losses and assure a fast response time (around 5 s). The PTR-MS inlet was not heated, but the analytes with low vapor pressure are produced by smoldering combustion during which the smoke temperature was normally 0–20 °C above ambient. The PTR-MS employs chemical ionization to measure volatile organic compounds (VOC) in real time [*Hansel et al.*, 1995; *Lindinger et al.*, 1998]. Briefly, the instrument features a hollow cathode ion source that produces H_3O^+ reactant ions from water vapor in the sample. The sample air then passes through a drift tube where VOC with proton affinities (PA) > PAH_2O are ionized by proton transfer reactions with the H_3O^+. The product ions are analyzed by a quadrupole mass spectrometer. Under favorable operating conditions less than 5% of the H_3O^+ ions react with VOC in the sample and the concentration of product ions in the sample can be calculated using equation (1),

$$[VOC - H^+] \cong [H_3O^+]_0[VOC]k_{VOC}t \qquad (1)$$

where $[H_3O^+]_0$ is the density of H_3O^+ ions in the absence of neutral reactants, k_{VOC} is the respective reaction rate constant for the proton transfer from H_3O^+ to the VOC and t is the reaction time, which depends on length, pressure (P = 2 hPa), and voltage (V = 600, E/N = 130 Td) of the drift tube. The reaction rate of most exothermic proton transfer reactions is nearly equal to the collision rate, and when specific reaction rates are unknown, they can be calculated [*Su and Chesnavich*, 1982]. For methanol, acetonitrile, acetone, and acetaldehyde the rate constants are known and the estimated accuracy of the mixing ratios is ±15–20% (2σ). The rate constants for these molecules are 2.2, 3, 3.4,

and 3.6 ($\times\ 10^{-9}$ cm^3 s^{-1}), respectively. For the other species (except HCHO) a rate constant of 2×10^{-9} cm^3 s^{-1} was used and the uncertainty in the mixing ratios should be ≤±50% with the estimate of the reaction rate constant (±30%) being the main source of error.

[9] During these experiments, the PTR-MS operated in either of two modes. In full mass scan mode the instrument was configured to scan incrementally from 17 to 142 atomic mass units, with a sample time of 20 ms per mass. In selected mass scan mode the instrument was configured to scan a selection of 30–36 masses, with a sample time of 0.1–0.2 s. Overall time resolution for either mode was about 4 to 8 s. The PTR-MS computer was synchronized with the rest of the data acquisition and the results were splined to match the OP-FTIR points.

[10] The strengths of PTR-MS [*Lindinger et al.*, 1998] include the following: (1) linear response up to ppm levels and ppt detection limits without preconcentration, which is adequate sensitivity for many species in clean air, (2) response to a wide variety of NMOC, including most OVOC, (3) fast measurement time (on the order of milliseconds) for an individual mass allowing rapid online monitoring of a single mass or sequential measurements of numerous masses repeated with high frequency, and (4) quickly available mixing ratios without complex analysis of spectra or chromatograms, even for unidentified species. Disadvantages of PTR-MS include the following: (1) measurements are limited to molecules with a proton affinity greater than that of water, (2) losses can occur on the sample line or within the instrument, and (3) species identification and quantification can be complicated by the presence of other compounds and fragments with the same mass to charge ratio. Fragmentation ratios can be measured for individual compounds, but, in practice, fragmentation of large, unidentified compounds could add unwanted signal to lower masses.

2.2.3. Canister Sampling

[11] Up to three evacuated stainless steel canisters could be simultaneously filled in $\sim$10 s to ambient pressure via a "cross" manifold and a 4 mm i.d. stainless steel sampling tube that opened next to the PTR-MS inlet. The sample line pressure was logged on the data system so that the filling time of these "quick cans" with respect to other instruments was precisely known. "Integrated" cans were filled at a preselected linear rate, over a precisely known period, through another collocated inlet. Forty integrated cans and 28 quick cans, taken before or during most fires, were analyzed by GC-FID for CO_2, CO, ethylene, acetylene, and propylene by the USDA Forest Service. Preconcentration was not used in the analysis of these cans and the system noise of $\sim$20 ppbv limited the typical accuracy to approximately ±5% for ethylene and approximately ±25% for propylene (2σ). The chromatographic error for acetylene is similar to that for the other compounds, but it is sometimes lost at $\sim$25% per month in the USFS cans (S. Baker, personal communication, 2002). Seven quick cans taken during the fires were analyzed at UC Irvine on a 5 column/detector analytical system (2 GC-FID, 1 GC-MS, and 2 GC-ECD) to obtain mixing ratios for 7 compounds that were also measured by either FTIR or PTR-MS: ethylene, propylene, acetylene, isoprene, benzene, toluene, and *p*-xylene. The uncertainty in these analyses is estimated to be <10% (2σ). All the cans were analyzed 2–3 months after collection.
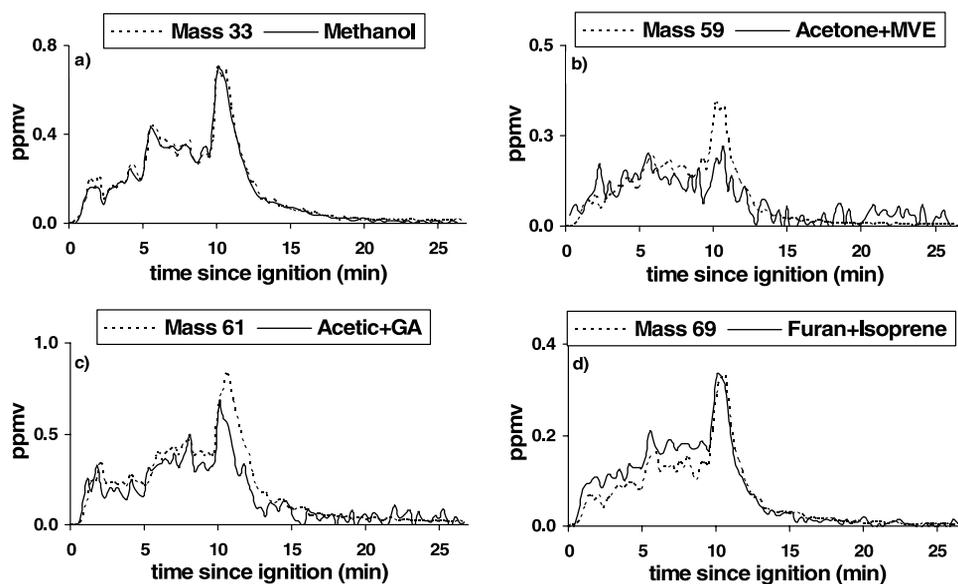
Figure 3. Typical agreement between the PTR-MS and OP-FTIR is illustrated by coplotting the real time excess mixing ratios from the two instruments. The above data were measured during the third fire in ponderosa pine needles. (a) Mass 33 (methanol); (b) mass 59 (acetone and methylvinylether); (c) mass 61 (acetic acid and glycolaldehyde); (d) mass 69 (furan and isoprene). GA, glycolaldehyde; MVE, methylvinylether.

Details about the canister analysis protocols are found elsewhere [*Hao et al.*, 1996; *Colman et al.*, 2001]. The chief advantages of canister sampling/GC analysis are: (1) accurate measurement of 50–100 "stable," nonsticky species down to 2–4 ppt levels if preconcentration is used, and (2) specificity based on retention time and/or mass spectrum identification. The chief disadvantages include the following: (1) the measurements are intermittent (high time resolution is impractical), (2) results are not immediately available, and (3) it is impossible to measure "unstable" or sticky molecules [*Kelly and Holdren*, 1995]. Uncertainty as to which compounds are unstable or sticky means that the accuracy of published canister sampling data, especially for OVOC, is not always clear. Since method development for OVOC analysis in canisters by the two groups in this study is ongoing, our canister comparisons are limited to NMHC.

2.2.4. Other Measurements

[12] The 19 mm inlet used for filling canisters at a linear rate also provided sample air for continuous CO_2 (LICOR 6262) and CO (TECO 48C) measurements. The TECO and both LICORs (including the background air monitor) were calibrated daily with NIST traceable standards. Stack air was drawn at 30 L min^{-1} through dielectric tubing to a cyclone to remove particles larger than 2.5 μm effective diameter, then onto Teflon or quartz filters analyzed as described by *Christian et al.* [2003]. We monitored fuel mass and stack temperature, pressure, and flow (Kurz model 455) with 2 s resolution.

3. Results and Discussion

[13] Figure 3a shows the excess mixing ratios (i.e., smoke minus background) for methanol measured by PTR-MS and OP-FTIR for a pine needle fire. Mixing ratios for this fire were typical of the experiments as a whole. We integrated

the methanol excess mixing ratios from the PTR-MS over the whole fire and divided that number by the integrated excess mixing ratios from the OP-FTIR (PTR-MS/OP-FTIR = 1.01). This is a straightforward method to quantify the agreement observed between PTR-MS and OP-FTIR: (1) It is insensitive to random noise and imperfect synchronization. (2) It should quantify the net effect of constant or temporary, positive or negative instrumental errors. (3) Differences in the integrated excess mixing ratios account for much of the uncertainty in the individual emission factors reported in the companion paper [*Christian et al.*, 2003].

[14] We also compare "quick" canister mixing ratios to the average mixing ratio measured by PTR-MS or OP-FTIR during the time each can was filled (as revealed by the pressure data for the canister sample line). The overall average ratio for stable light hydrocarbons for the UCI and USFS cans divided by the OP-FTIR is 1.01 ± 0.39, $n = 30$ (Table 1). The scatter is larger than observed in a previous test of the agreement between integrated cans and OP-FTIR [*Goode et al.*, 1999]. This suggests that differences up to ~0.4 between spot measurements can be expected, on average, from timing uncertainty, leaks, and instrumental uncertainties. Thus other factors probably contributed to the larger differences observed for some can/FT comparisons. For example, propylene concentration was changing rapidly during the Miombo2 fire while the cans were being filled.

3.1. Detailed Results Organized in Order of Ascending Mass

[15] The PTR-MS is designed to avoid ionizing trace gases with PA ≤ PAH$_2$O. This conveniently excludes some abundant gases such as N_2, CO_2, CO, H_2, O_2, etc. that would scavenge too many reactant ions and can be mea-

Table 1. Canister Mixing Ratios Divided by the Simultaneously Measured PTR-MS and OP-FTIR Mixing Ratios

UCI GC/MS-FID-ECD "Can" Compounds	Fire Name							Average All	Average Steady Fires[a]
	Alangalang4	IndoLitter1	Firduff3b	Dambo3	Miombo2	GermanGrass3	Miombo3		
Ethylene/FT[b]	0.91	1.45	0.67	0.95	0.75	1.14	1.01	0.98	1.06
Propylene/FT	0.74	0.99	0.73	nFT[c]	0.23	0.65	1.47	0.80	0.86
Acetylene/FT	0.97	1.79	0.87	1.19	1.18	1.66	1.43	1.30	1.33
Isoprene/PT m69[d]	0.0035	0.082	0.062	0.018	0.021	0.0038	0.0026	0.028	0.072
Benzene/PT	1.58	1.49	0.10	1.36	1.04	1.00	1.60	1.17	0.79
Toluene/PT	1.86	1.51	0.82	1.52	1.15	0.81	1.60	1.32	1.16
p-Xylene/PT m107[e]	0.10	0.68	0.38	nPT	0.30	0.17	0.74	0.40	0.53

USFS GC-FID "Can" Compounds	Fire Name							Average All	Average Steady Fires
	Alangalang4	IndoLitter1	Firduff3b	Dambo3	Miombo2	GermanGrass3	Miombo3		
Ethylene/FT	1.26	1.61	nC	0.72	0.96	1.28	nC	1.17	–
Propylene/FT	0.92	1.28	nC	nC	0.29	0.60	nC	0.77	–
Acetylene/FT	0.51	nC	nC	nC	nC	nC	nC	0.51	–

[a]The average of the ratios from the fires with slowly changing emissions.
[b]FT indicates the ratio of canister analysis to the OP-FTIR analysis, and PT indicates the ratio is to the PTR-MS analysis.
[c]Here, nFT, no FTIR data; nPT, no PTR-MS data; nC, no can data.
[d]Isoprene and furan both contribute to the PTR-MS mass 69 signal.
[e]PTR-MS mass 107 includes all xylenes.

sured by other means. The FTIR measured 7 trace gases with PA ≤ PAH2O - CO_2, CO, H_2O, CH_4, C_2H_2, C_2H_4, and NO. In this section we present a quantitative discussion of the agreement between PTR-MS, OP-FTIR, and canister sampling for gases with PA > PAH2O. We present the results in ascending order of the relevant PTR-MS mass channel. In the heading for some masses, we summarize the study-average agreement in parentheses. For example, the study-average for the integrated PTR-MS excess mixing ratios divided by the integrated OP-FTIR excess mixing ratios is abbreviated PT/FT. (The averages and the standard deviations (1σ) were computed after discarding the highest and lowest ratio for each compound and n indicates the number of fires used in the calculation.)

3.1.1. Mass 18, Ammonia

[16] Ammonia has a high proton affinity relative to water, but it readily sticks to certain surfaces [Yokelson et al., 2003b]. The PTR-MS exhibited a slow response for NH_3 (on the order of hours), which was probably due to passivation of metal surfaces within the instrument. The OP-FTIR is immune to sampling artifacts, the NH_3 S/N was high for all fires, and the IR spectral analysis by two different methods agreed well. As part of this work, Yokelson et al. [2003b] compared the NH_3 risetime in a fast flow, closed-cell FTIR system to that of nonsticky gases. Because of passivation of the Pyrex cell the NH_3 rise was delayed by 10–40 s, depending on flow rate.

3.1.2. Mass 28, HCN; and Mass 31, HCHO

[17] HCN and HCHO were detected by FTIR and PTR-MS. However, these compounds have a PA only slightly above that of H_2O and their protonation in the PTR-MS drift tube is strongly dependent on humidity. Accurate measurements of HCN and HCHO by PTR-MS would have required detailed calibration, with point-by-point corrections, over a broad range of relative humidities. Those calibrations were not done in this experiment. Hansel et al. [1997] recommended a rate constant and described a rough method to correct HCHO mixing ratios without calibration. Their method, applied to our experiment, sug-

gests multiplying the mixing ratios for HCHO by 4. We applied the same correction to HCN, since it has the same PA as HCHO. This correction results in study-average PT/FT ratios for HCN and HCHO of 0.34 and 1.33. Therefore we used the OP-FTIR results for these two trace gases in the companion paper by Christian et al. [2003].

3.1.3. Mass 33, Methanol (PT/FT = 1.04 ± 0.118, n = 38)

[18] As mentioned earlier, Figure 3a shows typical agreement between PTR-MS and OP-FTIR for methanol. This agreement was excellent for all the fires except the single miombo litter fire. The ratio for this fire (1.60) was not used in the calculation of the PT/FT ratio shown above. Because methanol is the second most abundant organic compound in the atmosphere after methane [Singh et al., 2001], and to ensure that the initial good agreement was not fortuitous because of an incorrect IR cross-section, we remeasured the methanol IR spectrum (and also that of ammonia and several other gases) with a high-accuracy apparatus described by Yokelson et al. [2003b]. This indicated that the methanol IR calibration was accurate to within a few percent. The good agreement for these two instruments is encouraging. We note that a recent airborne intercomparison of fast GC and PTR-MS in cleaner air showed poor agreement for methanol [Hansel et al., 2002].

3.1.4. Mass 42, Acetonitrile

[19] The IR cross-section for acetonitrile is small and we did not detect it in any FTIR spectra. The PTR-MS detected mass 42 in all fires. This mass is attributed to acetonitrile, as there are no other plausible, nonradical, nonionic candidates at this mass. Charge exchange reactions between three and four carbon alkanes and O_2^+ are known to produce fragments in the PTR-MS that contribute to the mass 42 signal. However, the O_2^+ abundance in the drift tube is less than a few percent of the H_3O^+ abundance and the charge exchange reactions are about one-half as fast as proton transfer to acetonitrile [Spanel and Smith, 1998]. Thus, in other studies, the alkane-derived contribution at mass 42 was "very minor" compared to the acetonitrile contribution, even when the alkane abundance in the sample was

approximately equal to that of acetonitrile [*de Gouw et al.*, 2003a; *Warneke et al.*, 2003]. Since the sum of alkanes measured by GC in smoke is only one half to one tenth of the mass 42 signal (Table 4 of *Christian et al.* [2003]), their contribution is insignificant in this work.

3.1.5. Mass 43, Propylene (PT/FT = 2.33 ± 0.89, *n* = 19; GC/FT = 0.79 ± 0.39, *n* = 10)

[20] The PTR-MS normally measured higher mixing ratios for mass 43 than the propylene mixing ratios measured by OP-FTIR. The OP-FTIR data for propylene from several fuel types, including African savanna fuels, was excluded from this comparison because of very low S/N. No other compounds with protonated mass 43 were detected by OP-FTIR (e.g., cyclopropane). Separate experiments showed that 30% of acetic acid (protonated mass 61) fragments to mass 43 in the PTR-MS. That is, some protonated acetic acid loses H_2O and forms CH_3CO^+. Other gases with protonated mass 61 can potentially contribute to mass 43 via similar mechanisms (e.g., glycolaldehyde to yield CH_3CO^+ or propanol to yield $C_3H_7^+$ [*Lindinger et al.*, 1998]), but their fragmentation was not measured and propanol was not observed by FTIR. A correction was made to the PTR-MS mass 43 data to account for fragmentation of mass 61 (which was primarily acetic acid with smaller amounts of glycolaldehyde). Specifically the raw ppb mass 61 was adjusted upward by 30% and the raw ppb mass 43 was decreased by 30% of the adjusted ppb mass 61. Table 1 compares propylene mixing ratios from the UCI and USFS quick cans to the average OP-FTIR propylene mixing ratio during the time that the cans were collected. Propylene by GC averaged about 80% of the OP-FTIR propylene. Since three groups obtained propylene values substantially lower than the mass 43 signal, it seems likely that a larger, as yet unidentified, species contributes to this mass channel via fragmentation.

3.1.6. Mass 45, Acetaldehyde

[21] Acetaldehyde has not been detected by FTIR in biomass burning emissions. However, the PTR-MS mass 45 signal for these fires was relatively high. CO_2 and N_2O have the same mass as acetaldehyde, but they have low proton affinities and are not detected by PTR-MS. We could not attribute any IR absorption lines to other mass 45 candidates (with PA > PA_{H_2O}) such as ethylene oxide. The isolated acetaldehyde features in the IR spectrum are too weak, even at the mixing ratios obtained in this study by PTR-MS, to be readily detectable by FTIR. Fast GC and PTR-MS agreed very well for acetaldehyde during TexAQS [*Hansel et al.*, 2002], but the acetaldehyde mixing ratios measured by GC-RGD (reduction gas detector) during TRACE-P were about one-half those measured simultaneously by fast GC-MS [*Eisele et al.*, 2003]. PTR-MS is probably the only way to measure acetaldehyde continuously.

3.1.7. Mass 47, Formic Acid (PT/FT = 0.417 ± 0.168, *n* = 38)

[22] The PTR-MS mass 47 signal accounted for only about half the formic acid measured by the OP-FTIR. Losses in the PTR-MS inlet are a likely problem for this sticky compound. Because a fast response was observed at this mass, the signal was probably due to some other, less sticky, mass 47 candidate(s) such as ethanol or dimethylether. However, neither of these was evident in the IR spectra.

3.1.8. Mass 54, Propenenitrile; and Mass 56, Propanenitrile

[23] Propenenitrile (C_3H_3N) seemed to be the only logical candidate for mass 54. Mass 56 was identified as propanenitrile (C_3H_5N), and included as such in the tables in the companion paper by *Christian et al.* [2003], mostly because its emission ratio to CO (0.023%) was similar to the propanenitrile/CO ratio reported by *Lobert et al.* [1991] (0.02%) when the comparison is restricted to fires in similar fuels (mostly grass and pine needles). Since fuel nitrogen is variable, this identification is admittedly weaker than the others in this work. No search for either of these compounds was made in the IR spectra because of the low levels observed.

3.1.9. Mass 59, Acetone, Methylvinylether (PT/FT = 1.29 ± 0.81, *n* = 29)

[24] The best IR peak for acetone is fairly broad, and it is overlapped by complex structure due to other compounds in smoke. As a result, the presence of acetone was obvious only in the IR spectra for one fuel type (rice straw). Because of its importance, we measured the acetone IR cross-section at four different pressures. Most of the fires emitted small, but detectable (by FTIR), amounts of methylvinylether, which is also a mass 59 candidate (Figure 3b). The FTIR ratio of acetone to methylvinylether was ∼6 for the fires with the highest S/N. The study-average ratio, which included fires with lower FTIR S/N, was 1.8 ± 1.9. (Natural variability among the different fuel types contributes to the high standard deviation.) These two gases are combined in the denominator of the PT/FT ratio shown above. The average PT/FT for both the dambo and miombo fires was <0.7, but for all other fuel types the average ratio was >1.0. We did not detect any other mass 59 candidates in any fire by FTIR, despite a concerted effort to identify the following compounds with reasonably strong and isolated IR peaks: propanal, trimethylene oxide, and propylene oxide. One other plausible mass 59 candidate is glyoxal, which has been identified as a major product of the fast pyrolysis of biomass [*Thamburaj*, 2000]. However, the glyoxal IR peaks that do not suffer from severe water interference are weak (T. Dransfield, personal communication, 2002). No glyoxal features were seen in the IR spectra from the fire with the highest mass 59 signal. From our glyoxal detection limit we can infer that glyoxal accounted for <20% of the mass 59 signal from this fire. We conclude that the signal at mass 59 in these fires is mostly acetone with smaller contributions by MVE and possibly glyoxal.

3.1.10. Mass 61, Acetic Acid, Glycolaldehyde (PT/FT = 1.17 ± 0.34, *n* = 39)

[25] Normally, within experimental uncertainty, all the PTR mass 61 signal is accounted for by acetic acid and its structural isomer glycolaldehyde, as determined by OP-FTIR (Figure 3c). The FTIR signal for acetic acid was strong for all fires and its average ratio to glycolaldehyde was 5.7 ± 3.4. As detailed in the section on mass 43, the mass 61 signal was corrected to account for fragmentation in the drift tube. In earlier PTR-MS smoke measurements acetic acid was lost on the inlet, but the fast response and good agreement suggest that this was overcome in this work by using a shorter, wider inlet. However, similar improvement was not observed for formic acid so it may be more prone to sampling losses.
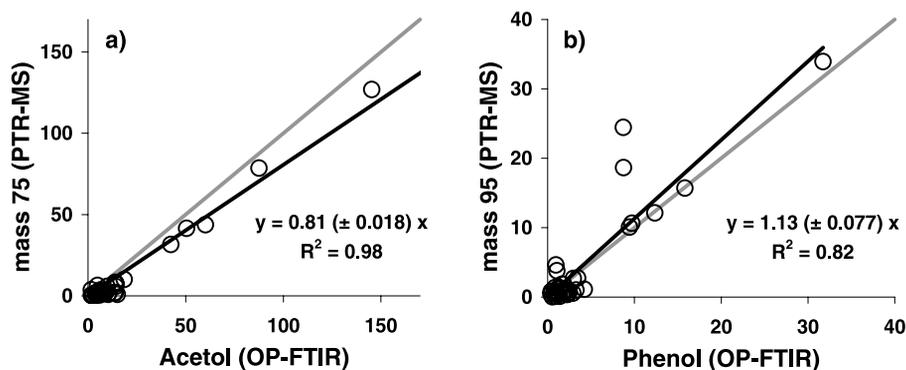
Figure 4. Regression of the PTR-MS fire-integrated excess mixing ratios against the OP-FTIR fire-integrated excess mixing ratios for all the fires. (The 1:1 ratio is shown as a gray line.) This is an alternative method to determine the study-average agreement between the instruments that is biased toward the agreement obtained for the fires with higher mixing ratios (see text). (a) For acetol and mass 75, good agreement is always obtained at high mixing ratios. (b) For phenol and mass 95, excellent agreement is observed on 5 of the 7 occasions with high mixing ratios. Another mass 95 candidate may contribute to the outliers.

3.1.11. Mass 69, Furan, Isoprene (PT/FT = 0.783 ± 0.465, n = 39)

[26] The IR spectral analysis for furan is complicated by CO_2 lines at high CO_2 (which occurred in roughly 40% of the fires), and extra care was needed to correctly retrieve furan. Isoprene was unaffected by high CO_2. The study-average sum of the furan and isoprene (by FTIR) is consistent with the PTR-MS mass 69 signal within experimental uncertainty (see individual fire in Figure 3d). The study-average furan to isoprene ratio by FTIR was 2.6 ± 2.6. The UCI group quantified isoprene but because they do not routinely measure OVOCs, they did not report furan concentrations. The UCI isoprene averaged <3% of the mass 69 simultaneously measured by PTR-MS. This is consistent with FTIR data collected at the time of these cans, which shows that most of the mass 69 was furan and that isoprene was at or below the FTIR detection limit when 6 of the 7 UCI cans were collected.

3.1.12. Mass 75, Acetol (PT/FT = 0.416 ± 0.289, n = 36; PT/FT = 0. 81 ± 0.018, Alternate Method)

[27] The rice straw fires emitted large amounts of acetol (hydroxyacetone), which is previously unreported in biomass burning emissions. The FTIR retrievals for acetol are based on our own careful measurement of the IR cross-section at five different concentrations. In the PTR-MS, acetol fragments to yield ~80% on mass 75, ~20% on mass 57, and <2% on mass 43. This fragmentation is accounted for in the PTR-MS retrieval. In theory, a low PT/FT ratio for a compound could arise because of inlet losses, low proton affinity, or fragmentation. However, acetol is not sticky, it has high PA, and the fragmentation has been accounted for. In this case, a remaining explanation for the low ratio could be low signal to noise in some of the data, most likely from the FTIR. In other words, the comparison procedure adopted above weights the ratio from all fires equally. This procedure is justified when good signal to noise is the norm, but could fail if ratios from fires with very poor S/N, and thus high error, are given too much weight in deriving the study average. As an alternative, we can plot the PTR-MS fire-integrated mixing ratios against the simultaneously measured OP-FTIR fire-integrated mixing ratios for all the fires. The slope of the linear regression line in such a plot gives an estimate of the study-average ratio that heavily weights the larger values, which correspond to higher S/N. While this procedure biases the study-average agreement toward the agreement obtained on fires that happened to have high signal levels, it is a valuable tool when other contributions to "low" ratios can be eliminated. We show such a plot for acetol in Figure 4a. The slope (0.81 ± 0.018), and lack of outliers, implies good agreement between OP-FTIR and PTR-MS whenever there were high signal levels. Similar plots were made to check the implications for other compounds, but, with one exception, they did not suggest a significantly different level of agreement. For mass 59, such a plot implies significantly worse agreement, which may rule out low FTIR S/N as the sole cause of the discrepancy.

3.1.13. Mass 79, Benzene (GC-UCI/PT ~1.2); Mass 93, Toluene (GC-UCI/PT ~1.3); and Mass 107, *p*-Xylene/ Xylenes (GC-UCI/PT ~0.4)

[28] In the UCI cans, good average agreement was obtained with PTR-MS for benzene and toluene (Table 1), which supports the single compound identification for these masses in this work. The GC-UCI/PT ratio for xylene of 0.4 could be due to one or more of the following: error in the PTR-MS rate constant, interference at mass 107 (e.g., other xylenes and ethyl benzene [*Warneke et al.*, 2001; *de Gouw et al.*, 2003b]), or small storage losses of xylene in these cans. Some previous storage tests found that the compounds discussed here were stable in cans, but both production and losses have also been observed in similar canisters during similar storage periods [*Schmidbauer and Oehme*, 1988; *Kelly and Holdren*, 1995; *Gong and Demerjian*, 1995; *Habram*, 1998; *Sin et al.*, 2001; *Ochiai et al.*, 2002]. These compounds are known, along with ethyl benzene, as "BTEX" compounds and they are of special interest in urban pollution studies. The UCI can method has advantages for measuring individual xylenes in smoke [*Ferek et al.*, 1998] while PTR-MS has the advantage of measuring benzene and toluene in real time.
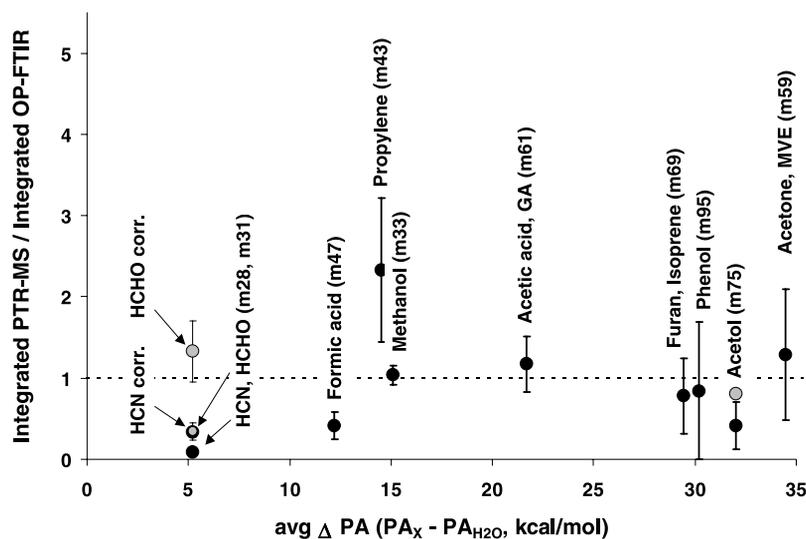
Figure 5. The x axis is the proton affinity (PA) of the compound minus the PA of water (ΔPA). The black symbols show the average value and 1 standard deviation for the fire-integrated PTR-MS excess mixing ratios divided by the fire-integrated OP-FTIR excess mixing ratios. The gray symbols show the agreement obtained after corrections for HCHO and HCN discussed in the text or from the alternate analysis for acetol shown in Figure 4a.

3.1.14. Mass 95, Phenol (PT/FT = 0.843 ± 0.845, n = 28)

[29] On average, within the combined uncertainty for the two instruments, all the PTR-MS mass 95 signal is accounted for by the OP-FTIR phenol, but the scatter is very high. The large scatter was mostly due to fires with lower FTIR S/N for phenol, but there was also evidence (at high S/N) of occasional contributions to the mass 95 signal from a long list of candidates with molecular mass of 94 that includes six with molecular formula C_6H_6O, 10 with formula $C_5H_6N_2$, 52 with formula C_7H_{10}, and candidates containing chlorine or sulfur. Vinyl furan could interfere with phenol at mass 95 and it has several strong, isolated IR peaks. However, no sign of vinyl furan was detected by FTIR even though it has been reported in canister analysis of smoke samples. No other mass 95 candidates were observed by OP-FTIR or in the canisters. In general, as molecular mass increases, the number of candidates for PTR-MS interference may grow and broader features may characterize the IR spectrum. Thus the larger species can be harder to measure and also more likely to partially partition into the condensed phase. Finally, to investigate the contribution of low S/N to the scatter we also made a plot using the procedure described above for mass 75. The plot, in Figure 4b, shows numerous low values near the intercept, 5 points at high levels that define a line with slope 1.02 ± 0.036, and two high concentration points that lie above the line and increase the slope to 1.13 ± 0.077. This suggests that the agreement was usually excellent at high signal levels, but that something else may have contributed to mass 95 on 2 of the 7 fires with the highest S/N.

3.2. Summary of Results by Proton Affinity

[30] As stated earlier, we found excellent agreement between FTIR and PTR-MS for methanol for all but one fire in this study and good overall agreement between cans and OP-FTIR. This suggests that larger differences that occurred for some other compounds were not due to incomplete mixing, sampling artifacts for "nonsticky" molecules, or instrument drift. Proton affinity is a key variable affecting detectability by PTR-MS. In Figure 5, for selected compounds, we show the study-average value of the integrated PTR-MS excess mixing ratios divided by the integrated FTIR excess mixing ratios. Error bars represent one standard deviation. The x axis is the difference in proton affinity between the compound of interest and water (ΔPA, kcal/mol). When two compounds were detected at the same PTR-MS mass, the average ΔPA is used. Where proton affinity is unknown, we estimated the value. In summary, at low ΔPA (HCHO and HCN) the ratio was much less than one because of the equilibrium between protonation and the back reaction. A simple correction described by *Hansel et al.* [1997] improved the agreement as shown. Sample line or internal losses (HCOOH and NH_3) and uncorrected fragmentation of the ion being monitored (not evident in this study) could lead to ratios below one even with ΔPA > 10. Ratios larger than one could result from fragmentation of larger molecules creating spurious signal for the ion being monitored. This may cause the ratio to be larger than one for mass 43 (propylene) since mass 43 is known to be a common fragment mass. Two or more nonfragment species with the same molecular mass will be detected on the same mass channel. In fact, the sum of two compounds detected by FTIR at mass 61 (acetic acid and glycolaldehyde) and mass 69 (furan and isoprene) agrees very well with the total PTR-MS signal. At mass 59, the sum of two FTIR compounds (acetone and methylvinylether) accounts for most of the PTR-MS signal. The shortfall could be due to unusually complex interference causing systematically low FTIR retrievals for acetone or the failure of FTIR to detect other mass 59 species. Smaller deviations from one (positive or negative) could occur from inaccuracy in the

calibration of either instrument. The large spread or standard deviation in the ratio, which is observed in some cases, is likely due to a combination of low FTIR S/N for several gases and changing concentrations of interfering species for PTR-MS.

3.3. Summary of Results by Agreement Obtained and Attributes of Continuous Instruments

[31] This section summarizes the reasons for choosing data from a specific real time instrument for inclusion in the companion paper [*Christian et al.*, 2003], which presents quantitative data from African and Indonesian biomass burning emissions.

3.3.1. FTIR and PTR-MS Similar

[32] For methanol only, we obtained agreement that was excellent for nearly all fires. The PTR-MS would have an advantage measuring methanol in clean air because of its better detection limits. The average agreement is good for PTR-MS mass 95 and FTIR phenol, but with high scatter. At high signal levels, the agreement was usually excellent, but occasionally appears to reflect contributions from other mass 95 candidates. For acetol the agreement was always good at high signal levels.

3.3.2. Sum of FTIR Signals Similar to PTR-MS

[33] This category includes PTR-MS masses 59, 61, and 69. The FTIR detected two compounds with molecular mass of 60: acetic acid and glycolaldehyde. Except for the rice straw fires, the PTR-MS mass 61 signal is explained by these two species with fairly low scatter. Acetone and methylvinylether are the only two candidates detected by FTIR for PTR-MS mass 59 and isoprene and furan are the only two candidates detected by FTIR for PTR-MS mass 69. On average, the agreement is good, but there is higher scatter. The FTIR data are likely preferred for determining individual compounds in complex mixtures at >10–20 ppb levels, but the PTR-MS data for the sum of the compounds may be more accurate. It is also the only choice for <ppb levels.

3.3.3. PTR-MS Preferred

[34] Compounds in this category have good signal to noise by PTR-MS, unlikely interference from other species with the same molecular mass, known fragmentation patterns (or known not to fragment), and no sampling losses. In addition, FTIR S/N for these compounds is poor. This category includes acetonitrile (mass 42), acetaldehyde (mass 45), propenenitrile (mass 54), benzene (mass 79), and toluene (mass 93). There were no detectable peaks in the FTIR spectra for these compounds, which are reliably detected by PTR-MS [*Holzinger et al.*, 1999; *de Gouw et al.*, 2003a, 2003b].

3.3.4. FTIR Preferred

[35] A few factors may cause gases to fall into this category: (1) Compounds with PA $\leq$ PAH_2O are not detected by PTR-MS. These include water, methane, ethylene, acetylene, CO_2, CO, and NO. Proton affinities for HCHO and HCN are only slighter greater than that of water, so the equilibrium between protonation and the back reaction must be included to quantify these gases with PTR-MS. (2) At mixing ratios above the ppm level the PTR-MS can suffer from depletion of the reagent ion while FTIR can analyze gases up to any level. (3) Ammonia and formic acid exhibited slow response in the PTR-MS because of reactivity and/or sticking to surfaces. (Similar problems could occur for acetic acid without appropriate caution.)

4. Conclusions

[36] This work confirmed that 70–80% of organic fire emissions from biomass burning are OVOC [*Christian et al.*, 2003], which is consistent with the domination of global atmospheric organic chemistry by OVOC. However, these experiments in smoke (a reactive and concentrated mixture) show that many OVOC are difficult to speciate in mixtures with current technology, especially at the levels desired for global characterization. We found excellent agreement between FTIR and PTR-MS for methanol and good average agreement for other alcohols for all fires in this study. Poor agreement was obtained for HCN, propylene, and formic acid. The sum of two compounds measured by FTIR agreed reasonably well with the PTR-MS signal at masses 59 (acetone and methylvinylether), 61 (acetic acid and glycolaldehyde), and 69 (furan and isoprene). We observed good overall agreement between FTIR and GC for ethylene, propylene, and acetylene, and between PTR-MS and GC-MS for benzene and toluene. Many OVOC measurements based on canister analysis have been reported [*Greenberg et al.*, 1984; *Kirstine et al.*, 1998; *Friedli et al.*, 2001], but problems measuring these species in canisters have also been reported [e.g., *Ochiai et al.*, 2002]. OVOC were not speciated in the canisters collected in this experiment. GC is well suited to measure many stable compounds and such results can provide important insights into the dynamics and chemical environment influencing all species [*Hobbs et al.*, 2003]. However, characterizing the most abundant organic constituents of the atmosphere, which includes reactive and stable species, may require developing a lower noise source for FTIR or finding a method to make the PTR-MS more selective. Perhaps the latter is more likely by increasing the specificity of the ionization or ion detection process or by increased use of isotope information. However, schemes to increase the selectivity of PTR-MS should ideally not decrease the ability to measure sticky or reactive species. Meanwhile, with a combination of instruments, we can measure the top 25 or so initial emissions from biomass burning and PTR-MS can provide highly sensitive measurements of acetonitrile, which is a good indicator of biomass burning. The PTR-MS measurement of acetonitrile is likely more accurate than the PTR-MS measurement of HCN, which has also been proposed as an indicator of biomass burning [*Lobert et al.*, 1991; *Li et al.*, 2000]. Because of variable fuel nitrogen, neither of these compounds is likely to serve as a true tracer for fires. Species with smoky odors might also be useful as biomass burning tracers. However, a list of compounds known to have smoky odors did not include species that we positively identified in this study. Acetone is an important HO$_x$ source that is subject to several potential interference problems. In this study, the FTIR data suggest that acetone accounted for ~60–70% of mass 59 on average and methylvinylether was the only interferent observed.

References

Albritton, D. L., F. C. Fehsenfeld, and A. F. Tuck (1990), Instrumental requirements for global atmospheric chemistry, *Science*, *250*, 75–81.

Andreae, M. O., and P. Merlet (2001), Emission of trace gases and aerosols from biomass burning, *Global Biogeochem. Cycles*, *15*, 955–966.

Blake, N. J., D. R. Blake, B. C. Sive, T. Y. Chen, F. S. Rowland, J. E. Collins, G. W. Sachse, and B. E. Anderson (1996), Biomass burning emissions and vertical distribution of atmospheric methyl halides and other reduced carbon gases in the South Atlantic region, *J. Geophys. Res.*, *101*, 24,151–24,164.

Brune, W. H., et al. (1998), Airborne in-situ OH and HO$_2$ observations in the cloud-free troposphere and lower stratosphere during SUCCESS, *Geophys. Res. Lett.*, *25*, 1701–1704.

Carter, W. P. L., A. C. Lloyd, J. L. Sprung, and J. N. Pitts Jr. (1979), Computer modeling of smog chamber data: Progress in validation of a detailed mechanism for the photooxidation of propene and n-butane in photochemical smog, *Int. J. Chem. Kinet.*, *11*, 45–101.

Chatfield, R. B., H. B. Singh, A. Fried, M. J. Evans, D. J. Jacob, D. Blake, B. Heikes, R. W. Talbot, and G. W. Sachse (2002), Oxygenated organic chemicals in the Pacific troposphere: Sources and chemical consequences, *Eos Trans. AGU*, *83*(47), Fall Meet. Suppl., F58.

Christian, T. J., B. Kleiss, R. J. Yokelson, R. Holzinger, P. J. Crutzen, W. M. Hao, B. H. Saharjo, and D. E. Ward (2003), Comprehensive laboratory measurements of biomass-burning emissions: 1. Emissions from Indonesian, African, and other fuels, *J. Geophys. Res.*, *108*(D23), 4719, doi:10.1029/2003JD003704.

Colman, J. J., A. L. Swanson, S. Meinardi, B. C. Sive, D. R. Blake, and F. S. Rowland, (2001), Description of the analysis of a wide range of volatile organic compounds in whole air samples collected during PEM-Tropics A and B, *Anal. Chem.*, *73*, 3723–3731.

de Gouw, J. A., C. Warneke, D. D. Parrish, J. S. Holloway, M. Trainer, and F. C. Fehsenfeld (2003a), Emission sources and ocean uptake of acetonitrile (CH$_3$CN) in the atmosphere, *J. Geophys. Res.*, *108*(D11), 4329, doi:10.1029/2002JD002897.

de Gouw, J., C. Warneke, T. Karl, G. Eerdekens, C. van der Veen, and R. Fall (2003b), Sensitivity and specificity of atmospheric trace gas detection by proton-transfer-reaction mass spectrometry, *Int. J. Mass Spectrom.*, *223–224*, 365–382.

Eisele, F. L., et al. (2003), Summary of measurement intercomparisons during TRACE-P, *J. Geophys. Res.*, *108*(D20), 8791, doi:10.1029/2002JD003167.

Ferek, R. J., J. S. Reid, P. V. Hobbs, D. R. Blake, and C. Liousse (1998), Emission factors of hydrocarbons, halocarbons, trace gases, and particles from biomass burning in Brazil, *J. Geophys. Res.*, *103*, 32,107–32,118.

Flocke, F., et al. (2002), Observations of PANs on board the NASA P-3 during TRACE-P, *Eos Trans. AGU*, *83*(47), Fall Meet. Suppl., F81.

Friedli, H. R., E. Atlas, V. R. Stroud, L. Giovanni, T. Campos, and L. F. Radke (2001), Volatile organic trace gases emitted from North American wildfires, *Global Biogeochem. Cycles*, *15*, 435–452.

Gong, Q., and K. L. Demerjian (1995), Hydrocarbon losses on a regenerated Nafion(R) dryer, *J. Air Waste Manage. Assoc.*, *45*, 490–493.

Goode, J. G., R. J. Yokelson, R. A. Susott, and D. E. Ward (1999), Trace gas emissions from laboratory biomass fires measured by Fourier transform infrared spectroscopy: Fires in grass and surface fuels, *J. Geophys. Res.*, *104*, 21,237–21,245.

Greenberg, J. P., P. R. Zimmerman, L. Heidt, and W. Pollock (1984), Hydrocarbon and carbon monoxide emissions from biomass burning in Brazil, *J. Geophys. Res.*, *89*, 1350–1354.

Griffith, D. W. T. (1996), Synthetic calibration and quantitative analysis of gas phase infrared spectra, *Appl. Spectrosc.*, *50*, 59–70.

Griffith, D. W. T., W. G. Mankin, M. T. Coffey, D. E. Ward, and A. Riebau (1991), FTIR remote sensing of biomass burning emissions of CO$_2$, CO, CH$_4$, CH$_2$O, NO, NO$_2$, NH$_3$ and N$_2$O, in *Global Biomass Burning: Atmospheric, Climatic, and Biospheric Implications*, edited by J. S. Levine, pp. 230–239, MIT Press, Cambridge, Mass.

Guenther, A., et al. (1995), A global model of natural volatile organic compound emissions, *J. Geophys. Res.*, *100*, 8873–8892.

Habram, M. (1998), Entwicklung einer gaschromatographischen Methode für die Bestimmung atmosphärischer C2–C9 Kohlenwasserstoffe, *Band 53-98*, Fraunhofer Inst. Atmos. Umweltforsch., Garmisch-Partenkirchen, Germany, March.

Hansel, A., A. Jordan, R. Holzinger, P. Prazeller, W. Vogel, and W. Lindinger (1995), Proton transfer reaction mass spectrometry: Online trace gas

analysis at the ppb level, *Int. J. Mass Spectrom. Ion Processes*, *150*, 609–619.

Hansel, A., W. Singer, A. Wisthaler, M. Schwarzmann, and W. Lindinger (1997), Energy dependencies of the proton transfer reactions H$_3$O$^+$ + CH$_2$O ↔ CH$_2$OH$^+$ + H$_2$O, *Int. J. Mass Spectrom. Ion Processes*, *167/168*, 697–703.

Hansel, A., A. Wisthaler, F. Flocke, A. Weinheimer, R. Fall, P. Goldan, G. Hübler, and F. C. Fehsenfeld (2002), An intercomparison of airborne VOC and PAN measurements, *Eos Trans. AGU*, *83*(47), Fall Meet. Suppl., F153.

Hanst, P. L., L. L. Spiller, D. M. Watts, J. W. Spence, and M. F. Miller (1975), Infrared measurement of fluorocarbons, carbon tetrachloride, carbonyl sulfide, and other atmospheric trace gases, *JAPCA*, *25*, 1220–1226.

Hao, W. M., D. E. Ward, G. Olbu, and S. P. Baker (1996), Emissions of CO$_2$, CO, and hydrocarbons from fires in diverse African savanna ecosystems, *J. Geophys. Res.*, *101*, 23,577–23,584.

Hobbs, P. V., P. Sinha, R. J. Yokelson, T. J. Christian, D. R. Blake, S. Gao, T. W. Kirchstetter, T. Novakov, and P. Pilewskie (2003), Evolution of gases and particles from a savanna fire in South Africa, *J. Geophys. Res.*, *108*(D13), 8485, doi:10.1029/2002JD002352.

Holzinger, R., C. Warneke, A. Hansel, A. Jordan, W. Lindinger, D. H. Scharffe, G. Schade, and P. J. Crutzen (1999), Biomass burning as a source of formaldehyde, acetaldehyde, methanol, acetone, acetonitrile, and hydrogen cyanide, *Geophys. Res. Lett.*, *26*, 1161–1164.

Holzinger, R., L. Sandoval-Soto, S. Rottenberger, P. J. Crutzen, and J. Kesselmeier (2000), Emissions of volatile organic compounds from *Quercus ilex* L. measured by proton transfer reaction mass spectrometry under different environmental conditions, *J. Geophys. Res.*, *105*, 20,573–20,579.

Kelly, T. J., and M. W. Holdren (1995), Applicability of canisters for sample storage in the determination of hazardous air pollutants, *Atmos. Environ.*, *29*, 2595–2608.

Kirstine, W., I. Galbally, Y. Ye, and M. Hooper (1998), Emissions of volatile organic compounds (primarily oxygenated species) from pasture, *J. Geophys. Res.*, *103*, 10,605–10,619.

König, G., M. Brunda, H. Puxbaum, C. N. Hewitt, S. C. Duckham, and J. Rudolph (1995), Relative contribution of oxygenated hydrocarbons to the total biogenic VOC emissions of selected mid-European agricultural and natural plant species, *Atmos. Environ.*, *29*, 861–874.

Li, Q. B., D. J. Jacob, I. Bey, R. M. Yantosca, Y. J. Zhao, Y. Kondo, and J. Notholt (2000), Atmospheric hydrogen cyanide (HCN): Biomass burning source, ocean sink?, *Geophys. Res. Lett.*, *27*, 357–360.

Lindinger, W., A. Hansel, and A. Jordan (1998), On-line monitoring of volatile organic compounds at pptv levels by means of proton transfer mass spectrometry (PTR-MS): Medical applications, food control and environmental research (review), *Int. J. Mass Spetrom. Ion Processes*, *173*, 191–241.

Lobert, J. M., D. H. Scharffe, W. M. Hao, T. A. Kuhlbusch, R. Seuwen, P. Warneck, and P. J. Crutzen (1991), Experimental evaluation of biomass burning emissions: Nitrogen and carbon containing compounds, in *Global Biomass Burning: Atmospheric, Climatic, and Biospheric Implications*, edited by J. S. Levine, pp. 289–304, MIT Press, Cambridge, Mass.

Mason, S. A., R. J. Field, R. J. Yokelson, M. A. Kochivar, M. R. Tinsley, D. E. Ward, and W. M. Hao (2001), Complex effects arising in smoke plume simulations due to inclusion of direct emissions of oxygenated organic species from biomass combustion, *J. Geophys. Res.*, *106*, 12,527–12,539.

McKeen, S. A., T. Gierczak, J. B. Burkholder, P. O. Wennberg, T. F. Hanisco, E. R. Keim, R.-S. Gao, S. C. Liu, A. R. Ravishankara, and D. W. Fahey (1997), The photochemistry of acetone in the upper troposphere: A source of odd-hydrogen radicals, *Geophys. Res. Lett.*, *24*, 3177–3180.

McRae, G. J., and J. H. Seinfeld (1983), Development of a second generation mathematical model for urban air pollution: II. Evaluation of model performance, *Atmos. Environ.*, *17*, 501–523.

Montzka, S. A., R. C. Myers, J. H. Butler, J. W. Elkins, and S. O. Cummings (1993), Global tropospheric distribution and calibration scale of HCFC-22, *Geophys. Res. Lett.*, *20*, 703–706.

Mount, G. H., and E. J. Williams (1997), An overview of the tropospheric OH photochemistry experiment, Fritz Peak/Idaho Hill, Colorado, fall 1993, *J. Geophys. Res.*, *102*, 6171–6186.

Ochiai, N., A. Tsuji, N. Nakamura, S. Daishima, and D. B. Cardin (2002), Stabilities of 58 organic compounds in fused-silica-lined and SUMMA polished canisters under various humidified conditions, *J. Environ. Monit.*, *4*, 879–889.

Schade, G. W., and A. H. Goldstein (2001), Fluxes of oxygenated volatile organic compounds from a ponderosa pine plantation, *J. Geophys. Res.*, *106*, 3111–3123.

Schimel, D., I. G. Enting, M. Heimaann, T. M. L. Wigley, D. Raynaud, D. Alves, and U. Siegenthaler (1995), CO_2 and the carbon cycle, in *Climate Change 1994: Radiative Forcing of Climate Change and an Evaluation of the IPCC IS92 Emission Scenarios*, edited by J. T. Houghton et al., pp. 35–71, Cambridge Univ. Press, New York.

Schmidbauer, N., and M. Oehme (1988), Comparison of solid adsorbent and stainless-steel canister sampling for very low ppt-concentrations of aromatic-compounds (greater-than-or-equal-to-C-6) in ambient air from remote areas, *Fresenius Z. Anal. Chem.*, *331*, 14–19.

Sin, D. W., Y. C. Wong, W. C. Sham, and D. Wang (2001), Development of an analytical technique and stability evaluation of 143 C_3-C_{12} volatile organic compounds in Summa canisters by gas chromatography-mass spectrometry, *Analyst*, *126*, 310–321.

Singh, H. B., M. Kanakidou, P. J. Crutzen, and D. J. Jacob (1995), High concentrations and photochemical fate of oxygenated hydrocarbons in the global troposphere, *Nature*, *378*, 50–54.

Singh, H., Y. Chen, A. Staudt, D. Jacob, D. Blake, B. Heikes, and J. Snow (2001), Evidence from the Pacific troposphere for large global sources of oxygenated organic compounds, *Nature*, *410*, 1078–1081.

Spanel, P., and D. Smith (1998), Selected ion flow tube studies of the reactions of H_3O^+, NO^+, and O_2^+ with several aromatic and aliphatic hydrocarbons, *Int. J. Mass Spectrom.*, *181*, 1–10.

Staudt, A. C., D. J. Jacob, F. Ravetta, J. A. Logan, D. Bachiochi, T. N. Krishnamurti, S. Sandholm, B. Ridley, H. B. Singh, and B. Talbot (2003), Sources and chemistry of nitrogen oxides over the tropical Pacific, *J. Geophys. Res.*, *108*(D2), 8239, doi:10.1029/2002JD002139.

Su, T., and W. J. Chesnavich (1982), Parameterization of the ion-polar molecule collision rate constant by trajectory calculations, *J. Chem. Phys.*, *76*, 5183–5185.

Thamburaj, R. (2000), Fast pyrolysis of biomass for green power generation, paper presented at First World Conference on Biomass for Energy and Industry, Energia TA, Seville, Spain.

Warneke, C., C. van der Veen, S. Luxembourg, J. A. de Gouw, and A. Kok (2001), Measurements of benzene and toluene in ambient air using proton-transfer-reaction mass spectrometry: Calibration, humidity dependence, and field intercomparison, *Int. J. Mass Spectrom.*, *207*, 167–182.

Warneke, C., J. A. de Gouw, W. C. Kuster, P. D. Goldan, and R. Fall (2003), Validation of atmospheric VOC measurements by proton-transfer reaction mass spectrometry using a gas-chromatographic preseparation method, *Environ. Sci. Technol.*, *37*, 2494–2501.

Worden, H., R. Beer, and C. P. Rinsland (1997), Airborne infrared spectroscopy of 1994 western wildfires, *J. Geophys. Res.*, *102*, 1287–1299.

Yokelson, R. J., and I. T. Bertschi (2002), Vibrational spectroscopy in the study of fires, in *Handbook of Vibrational Spectroscopy*, edited by J. M. Chalmers and P. R. Griffiths, pp. 2879–2886, John Wiley, New York.

Yokelson, R. J., D. W. T. Griffith, and D. E. Ward (1996), Open-path Fourier transform infrared studies of large-scale laboratory biomass fires, *J. Geophys Res.*, *101*, 21,067–21,080.

Yokelson, R. J., D. E. Ward, R. A. Susott, J. Reardon, and D. W. T. Griffith (1997), Emissions from smoldering combustion of biomass measured by open-path Fourier transform infrared spectroscopy, *J. Geophys. Res.*, *102*, 18,865–18,877.

Yokelson, R. J., J. G. Goode, I. Bertschi, R. A. Susott, R. E. Babbitt, D. E. Ward, W. M. Hao, D. D. Wade, and D. W. T. Griffith (1999), Emissions of formaldehyde, acetic acid, methanol, and other trace gases from biomass fires in North Carolina measured by airborne Fourier transform infrared spectroscopy (AFTIR), *J. Geophys. Res.*, *104*, 30,109–30,125.

Yokelson, R. J., I. T. Bertschi, T. J. Christian, P. V. Hobbs, D. E. Ward, and W. M. Hao (2003a), Trace gas measurements in nascent, aged, and cloud-processed smoke from African savanna fires by airborne Fourier transform infrared spectroscopy (AFTIR), *J. Geophys. Res.*, *108*(D13), 8478, doi:10.1029/2002JD002322.

Yokelson, R. J., T. J. Christian, I. T. Bertschi, and R. A. Susott (2003b), Evaluation of adsorption effects on measurements of ammonia, acetic acid, and methanol, *J. Geophys. Res.*, *108*(D20), 4649, doi:10.1029/2003JD003549.

————————————

D. R. Blake, Department of Chemistry, University of California, Irvine, 516 Rowland Hall, Irvine, CA 92697-2025, USA. (drblake@uci.edu)

T. J. Christian and R. J. Yokelson, Department of Chemistry, University of Montana, Missoula, MT 59812, USA. (ted.christian@umontana.edu; byok@selway.umt.edu)

P. J. Crutzen and B. Kleiss, Atmospheric Chemistry Department, Max Planck Institute for Chemistry, Joh.-J.-Becher-Weg 27, Universitätscampus, D-55128 Mainz, Germany. (air@mpch-mainz.mpg.de; kleiss@mpch-mainz.mpg.de)

W. M. Hao, Fire Sciences Laboratory, USDA Forest Service, P. O. Box 8089, Missoula, MT 59807, USA. (whao@fs.fed.us)

R. Holzinger, Department of Environmental Science, Policy and Management, University of California, Berkeley, 151 Hilgard Hall, Berkeley, CA 94720-3110, USA. (holzing@nature.berkeley.edu)

T. Shirai, Earth Observation Research Center, Japan Aerospace Exploration Agency, Ohsawa 2-21-1, Mitaka, Tokyo 181-8588, Japan. (t.shirai@nao.ac.jp)